MICROSCOPY

Microscopy, 2017, 110–119
doi: 10.1093/jmicro/dfw110
Advance Access Publication Date: 2 January 2017

Article

Simultaneous imaging of multiple cellular events using high-accuracy fluorescence polarization microscopy

Sang-Yeob Kim[1,6†], Yoshiyuki Arai[2,†], Tomomi Tani[1], Hirofumi Takatsuka[3], Yoshiharu Saito[3], Takayuki Kawashima[4], Shojiro Kawakami[4], Atsushi Miyawaki[5], and Takeharu Nagai[2,*]

[1]Laboratory for Nanosystems Physiology, Research Institute for Electronic Science, Hokkaido University, Kita 20, Nishi 10, Kita-ku, Sapporo, Hokkaido 001-0020, Japan, [2]The Institute of Scientific and Industrial Research, Osaka University, 8-1 Mihogaoka, Ibaraki, Osaka 567-0047, Japan, [3]Scientific Solutions Product Development Division, Product Development Department, Olympus Corporation, 2951 Ishikawa-cho, Hachijoji-shi, Tokyo 192-8507, Japan, [4]Photonic Lattice, Inc., ICR 2F, 6-6-3 Minami-Yoshinari, Aoba, Sendai, Miyagi 989-3204, Japan, and [5]Laboratory for Cell Function and Dynamics, Brain Science Institute, RIKEN, 2-1 Hirosawa, Wako, Saitama 351-0198, Japan

[*]To whom correspondence should be addressed. E-mail: ng1@sanken.osaka-u.ac.jp
[†]These authors contributed equally to this work.
[6]Present Address: Department of Convergence Medicine, University of Ulsan College of Medicine & ASAN Institute for Life Sciences, ASAN Medical Center, Seoul, Republic of Korea, 88, Olympic-ro 43-gil, Songpa-gu, Seoul, 138-736, Korea

Received 30 August 2016; Editorial Decision 9 December 2016; Accepted 16 December 2016

Abstract

Förster resonance energy transfer (FRET) has been widely used to design indicators for biomolecules. Conventional FRET-based indicators enable quantitative measurements of analyzes by calculating the ratio between donor and acceptor fluorophores. However, such 'hetero-FRET'–based indicators, which use multiple differently colored fluorophores, restrict the simultaneous use of other colors of fluorescent molecules. To overcome this problem, we developed a 'homo-FRET'–based Ca^{2+} indicator, W-Cameleon, composed of two identical yellow fluorescent proteins. The binding of Ca^{2+} to the indicator induces a change in FRET efficiency, which in turn transforms into changes in fluorescence anisotropy. Given that the fluorescence polarization is depolarized by light passing through a high numerical aperture lens and reflecting on a dichroic mirror, we also developed a microscopy technique that reliably detects fluorescence anisotropy with high precision. Our design is aided by photonic-crystal technology, to compensate for the fluorescence depolarization. We thereby succeeded in the simultaneous visualization of three individual intracellular events by using three different fluorescent indicators. Our system may contribute to an expansion of the number of events that can be observed, which will enable a more quantitative understanding of biological phenomena.

Key words: fluorescence anisotropy, FRET, photonic crystals, polarization microscopy

Introduction

Multi-dimensional measurement of biological activities is important to quantitatively understand the biological systems in living cells. A pallet of fluorescent indicators, especially those based on genetically encoded fluorescent proteins, are considered to be useful tools, for investigation of biological phenomena in living cells in real time. Intensiometric and ratiometric are two types of indicators that already exist. The intensiometric type uses only one color to sense the dynamics of interest. For example, the color pallet of GECO series easily enables simultaneous multiple imaging of Ca^{2+}, in different cellular organelles [1]. However, the variability of expression levels among cells, makes it difficult to compare and quantify the signals, in different cells with different probes within the same culture plate. On the other hand, ratiometric type indicators, such as the YC-Cameleon series, use two fluorescent proteins, cyan fluorescent protein (CFP) and yellow fluorescent protein (YFP) [2]. If those two fluorescent proteins are expressed in the cell in an equimolar ratio, by fusion or using the *Thosea asigna* virus 2A peptide system [3], then the ratio of the two fluorescence proteins becomes independent of the expression levels. However, the measurement, of two different fluorescent colors, limits the use of multi-dimensional imaging in a visible wavelength. Therefore, development of a single color and ratiometric type indicator is desired for multi-dimensional imaging.

Many ratiometric type indicators utilize Förster resonance energy transfer (FRET), to sense physiological events as a change in FRET efficiency [4]. FRET requires two fluorescent probes, a donor and an acceptor, that have spectral overlap between donor emission and acceptor absorption. Thus, FRET occurs even with a pair of identical donor and acceptor, which is called 'homo-FRET' [5]. When the donor and the acceptor are far enough, so that FRET does not occur; the polarization of donor and acceptor emission light is parallel to the polarization of the excitation light. However, if FRET occurs between the fluorophores, then depolarization of acceptor emission against polarized excitation light is observed. FRET occurs as a result of the different geometric orientations of donor and acceptor, which is due to the packing of the whole structure of the probe. Calculation of fluorescence anisotropy can be used to evaluate how polarization of emission light is canceled. Fluorescence anisotropy is calculated by the parallel and perpendicular polarization components of emission light, against the polarization of excitation light. Thus, ratiometric observation can be achieved, by using homo-FRET-based probes. Homo-FRET has been used to study protein dynamics, oligomerization and association of membrane proteins on the cell surface [6–9]. Additionally, fluorescence anisotropy decay microscopy and red-edge anisotropy microscopy have been implemented, for steady-state fluorescence anisotropy imaging, to detect homo-FRET in live cells [9,10].

Measurement of anisotropy, like spectroscopic measurement, uses polarized light for the excitation and measurement of parallel and perpendicular emission of light, through polarizers on fluorescence microscopy [11]. However, there are two problems with polarization measurement, using conventional epi-fluorescent microscopy. A high numerical aperture (NA) objective lens, which is often used in high-spatial and high magnification imaging, alters the angle of linear polarization of light [12]. A dichroic mirror, which enables the separation of excitation and emission light, alters the linear polarized light to ellipsoidal polarized light, because of the multilayered metal ion membranes. This leads to depolarization of light and reduced accuracy of fluorescence anisotropy measurement. Sinya Inoué developed the rectifier, to solve the depolarization effect of high NA objective lens; it can compensate for the depolarization effect of high NA objective lens [13]. However, the rectifier only compensates for rotation of the polarization, by objective lens; thus, ellipsoidal cannot be compensated due to the anti-reflection coating. Therefore, the lens for the rectifier should be non-coated, which would be unsuitable for fluorescence observation. Thus, the rectifier cannot be used in current standard fluorescence microscopy. A new technique should be developed to overcome the depolarization effect, with use of an infinite conjugation optical system. Recently, a photonic crystal, which is a new optics with high-dimensional fabrication of nano-structure, enables modulation of the spatially heterogeneous polarized light [14]. Thus, the use of a specially designed photonic crystal can overcome the depolarization problem, in an infinite conjugate optical system. In this study, we report the development of calcium ion indicators, based on the homo-FRET, and the development of a polarization microscope in an infinite conjugate optical system.

Materials and methods

Gene construction

The C-terminally deleted Venus cDNA was amplified by PCR, using primers that incorporated a *BamH*I restriction site at the 5′ end and a *Sph*I restriction site at the 3′ end.

The restriction enzyme sites were activated on the amplified product, which was then ligated into the *BamHI*/*Sph*I sites of YC3.60; this produced VenusΔ11-CaM-M13-cp173Venus (Supplementary data Fig. S1a). The N-terminus of CaM-M13 cDNA was amplified by PCR, using a sense primer that incorporated 5′*BamH*I-*Sph*I restriction sites at the CaM-M13 N-terminus and reverse primers that added *Bgl*II-*Xho*I restriction sites after CaM-M13 amino acid residue 41. CaM-M13 cDNA, from amino acid residue 42 to the C-terminus, was amplified in a PCR reaction, which added an *Xho*I restriction site to the 5′ end and *Sac*I-*Eco*RI sites to the 3′ end. The N-terminal fragment 5′*BamH*I and 3′ *Xho*I restriction enzyme sites were activated, while the C-terminal fragment *Xho*I and *Eco*RI sites were activated. The two fragments were ligated into the *BamHI*/*Eco*RI cloning sites in the pRSET$_B$ vector (Invitrogen, MA, USA). The Venus cDNA, containing the sequence encoding the linker (GGSGG) at each terminus, was amplified by PCR. The 5′ primer incorporated a *BamH*I restriction site, while the 3′ primer added a *Sal*I restriction site. The restricted products were inserted into the CaM-M13 *Bgl*II/*Xho*I sites, including these restriction enzyme sites, to generate 41-Venus-CaM-M13. The cDNAs of Venus were amplified in a PCR reaction, using primers that incorporated 5′ *SacI* and 3′ *EcoRI* restriction enzyme sites. The restricted products were inserted into the *SacI*/*Eco*RI sites of 41-Venus-CaM-M13 to generate 41-Venus-CaM-M13-Venus, i.e. W-Cameleon (Supplementary data Fig. S1b). The construct was subcloned into pcDNA3 (Invitrogen), for mammalian expression. The GFP gene of the myristoylated alanine-rich PKC substrate (MARCKS)-GFP construct (a kind gift of N. Saito) was replaced with the mSECFP gene. The construction of protein kinase C gamma (PKC-γ)-DsRedT3 was reported previously [15].

Protein purification and *in vitro* spectroscopy

Recombinant W-Cameleon was expressed in *Escherichia coli* (JM109(DE3)) and purified, as described previously [2]. Steady-state fluorescence anisotropy was measured, using a fluorescence spectrometer (FP-715, JASCO, Tokyo, Japan), with an excitation wavelength of 510 nm and an emission wavelength of 540 nm. Ca^{2+}-free or Ca^{2+}-saturated buffers were prepared, by using O,O′bis (2-aminoethyl) ethyleneglycol- N, N, N′, N′ tetraacetic acid, as described previously [2].

Cell culture and transfections

HeLa cells were cultured on collagen-coated 35-mm glass dishes. The adherent cells were transfected with constructs, using SuperFect (QIAGEN, CA, USA), in accordance with the manufacturer's instructions. One microgram of DNA of MARCKS and PKC-γ, and 2 μg of W-Cameleon DNA were used to transfect HeLa cells cultured in 35 mm glass bottom dish with 70% confluent. The transfected cells were cultured for 1–2 days before observations were made.

Design of photonic crystal analyzers

The polarization performance, of the test objective lens, was measured by the system shown in Supplementary data Fig. S2. Two objectives lens, which had the same specifications, were positioned face to face. Both objective lenses were strain free 60× N.A. 1.35 (UPLSAPO60XO, Olympus, Tokyo, Japan). The collimated light, from a xenon lamp (UXL-75XB, USHIO, Tokyo, Japan), was transmitted through a narrow band filter (490–500 nm) and a polarizer. The on-axis incident light entered in the first objective lens. The light was focused by the first objective lens and then collected and collimated by the second objective lens. The collimated light was transmitted to a $\lambda/4$ phase plate and analyzer. Finally, the pupil planes of two objective lenses were focused on the charge-coupled device (CCD) chip plane. Figure 2a shows the pupil image of two UPLSAPO60XO objective lens on the CCD chip, when the polarized angle of the polarizer was perpendicular to the analyzer and the fast axis angle of the $\lambda/4$ plate was parallel to the polarizer. Ideally, the pupil image becomes dark at all points, if the polarization performance is not modulated by the two objective lenses. However, the pupil image did not become dark, because the polarization performance was modulated by the refractions at lens surfaces in two objective lens (Fig. 2a). We were able to measure the polarization performance of these objective lenses on pupil plane, by rotating the $\lambda/4$ plate and the analyzer. We measured the rotated angle α of $\lambda/4$ plate, at each white color point (Fig. 2a) and rotated analyzer angle ($\alpha + \beta$), where the brightness at this point reached minimum intensity. α is the polarization angle and β is the ellipsoid angle (Supplementary data Fig. S3). The polarization angle and the ellipsoid angle, on the pupil of a single objective (UPLSAPO60XO), were half the value of the measured data, as shown in Supplementary data Fig. S4.

Setup of homo-FRET microscopy

W setup the polarization microscopy, with an inverted microscope (IX81, Olympus), for anisotropy imaging. A mercury arc lamp provided trans-illumination, instead of epi-illumination, to avoid the depolarization effect by using dichroic mirrors. The microscope was equipped with mechanical shutters, a motorized filter changer for excitation filters (IX2, Olympus), a high speed filter wheel for emission

filters (Lambda 10-2, Sutter Instruments, Novato, CA) and a high speed filter wheel (Proscan II, Prior Scientific, MA, USA), at the bottom of the microscope, for photonic crystal analyzers. Excitation and emission filter pairs for W-Cameleon, MARCKS-mSECFP and PKC-γ-DsRedT3 were FF01-472/30-25 and FF01-542/27-25 (Semrock, NY, USA), FF01-438/24-25 and FF01-483/32-25 (Semrock), and FF01-542/27-25 and XF3090 (Omega Optical), respectively. The images of the parallel and perpendicular polarized emission light were observed by NA 1.40, 60× oil immersion objective lens (Olympus), with an electron-multiply CCD camera (DU-897E, Andor Technology). The microscope system was controlled by Metamorph software (Molecular Devices, CA, USA).

Anisotropy imaging

Fluorescence anisotropy (r), for each anisotropy measurement, was determined, by measuring the emission intensity through cross (I_{VH}) and parallel (I_{VV}) oriented polarizers, where the subscripts of the first and the second characters indicate the direction of polarizer and analyzer, respectively. The anisotropy was then calculated by $r = (G \cdot I_{VV} - I_{VH})/(G \cdot I_{VV} + 2\ I_{VH})$, where G is a compensation factor derived from the different polarization dependencies of the detector. G factors (= 1.2 in our system) were determined, by acquiring the ratio of the intensities at parallel and perpendicular orientations for a fluorescence in solution, with a steady-state anisotropy that should be close to zero. Total intensity and anisotropy images were measured and constructed by Metamorph (Molecular Devices). The ratio R = (*fluorescence intensity of plasma membrane − fluorescence intensity of cytosol*)/(*fluorescence intensity of cytosol*) was calculated, to determine the distribution of MARCKS-mSECFP and PKC-γ-DsRedT3, as representing the relative increase or decrease in the plasma membrane fluorescence intensity over the cytosol.

Results

Development of homo-FRET-based Ca^{2+} indicator

First, we investigated efficient homo-FRET pairs, by calculating the Förster radius R_0 and overlap integral $J(\lambda)$ of a pair of GFPs or Venus proteins, which indicate the small stokes shift. We set the orientation factor κ^2 to 2/3, as free rotational movement, to calculate these values. The calculated R_0 and $J(\lambda)$ values, obtained from the overlap of the absorption and emission spectra of Venus, were 5.5 nm and $1.58 \times 10^{-13}\,M^{-1}\,cm^3$, respectively (Fig. 1a). On the other hand, the parameters of eGFP were 5.0 nm and $0.86 \times 10^{-13}\,M^{-1}\,cm^3$. Therefore, we chose Venus, the brightest YFP, as the homo-FRET pairs for further study.

Next, we constructed a homo-FRET-based Ca^{2+} indicator, YY3.60, by replacing the eCFP moiety of a Venus with a C-terminal 11-amino-acid truncation (Supplementary data Fig. S1a); this was the same as in YC3.60, since YC3.60 showed large anisotropy change [2]. The anisotropy values for YC3.60 were 0.020 and 0.160, with and without Ca^{2+}, respectively, while the values for YY3.60 were 0.152 and 0.154. Thus, we investigated favorable positions for improving YY3.60. Kajihara *et al.* showed that a substantial calmodulin FRET change occurred, with the donor (BODIPY-FL) at amino acid residue Gly41 and the acceptor (BODIPY558) at the N-terminus [16]. Therefore, we inserted Venus into calmodulin residues Gly41 and Gln42, using polypeptide linkers GGSGG (41-Venus-CaM-M13). A Venus was connected to the C-terminus of 41-Venus-CaM-M13 (Fig. 1b and Supplementary data Fig. S1b).

Remarkably, 41-Venus-CaM-M13-Venus had a substantial anisotropy change, from 0.184 to 0.264 at zero and saturating Ca^{2+} concentrations, respectively; the data suggested a geometric conformational change (Fig. 1c and d). Thus, we named this chimeric protein 'W-Cameleon' for homo-FRET-Ca^{2+} indicator. Ca^{2+} titration measurements indicated that the W-Cameleon dissociation constant K_d and Hill's constant were 1.56 μM and 2.81, respectively (Fig. 1d).

Design of photonic crystal analyzers

Depolarization, by high NA objective lens, reduces the accuracy of polarization measurement. In fact, the polarizer and the analyzer are placed perpendicularly, when polarized light passes through the high NA objective lens; the light that passes through the analyzer is not blocked at the peripheral area (Fig. 2a). We needed to measure fluorescent anisotropy, with precision. Thus, we developed fluorescence polarization microscopy, with high NA objective lens. First, we measured the performance of high NA objective lens. The depolarization effect became more significant, as NA increased (Fig. 2a). We fabricated photonic crystal-based analyzers, to compensate for the effect (Fig. 2b). We assumed a light beam, whose local state of polarization is shown in Supplementary data Fig. S4. First, we transformed it to a linearly polarized light, with a spatially changing direction of polarization. This was achieved by using a quarter-wave plate (QWP), with the fast axis forming an angle α with respect to the polarizer axis. We then led it to a polarizer (analyzer), with the local extinction axis forming the angle $(\alpha + \beta)$ to form a perfect extinction. All optical rays were blocked, except for those arising by polarization conversion at a specimen. We needed a QWP and a polarizer, whose principal axes can be arbitrarily curved. Such components can be fabricated in the

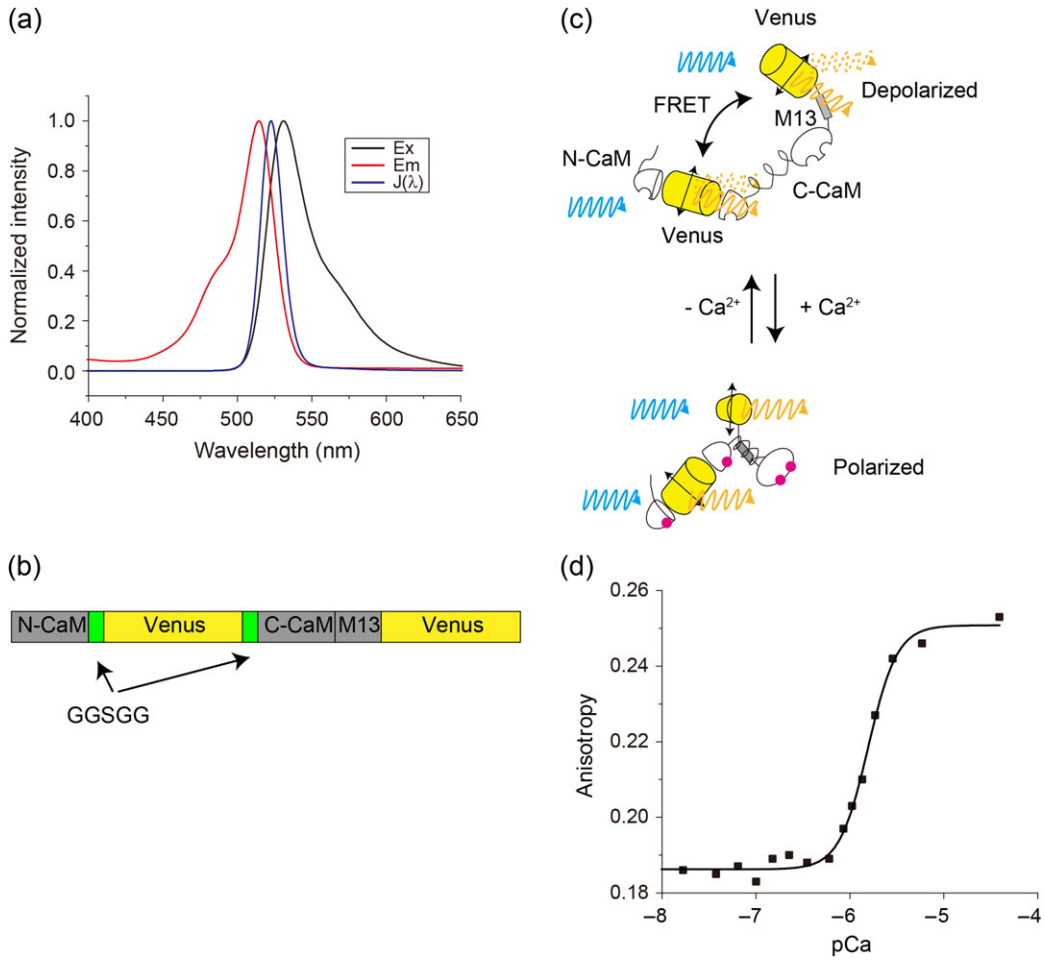

Fig. 1. Homo-FRET Ca^{2+} indicator, W-Cameleon. (a) Normalized absorption and emission spectra of YFP and the overlap integral. (b) Schematic sequence of W-Cameleon. (c) Conformational change of W-Cameleon, with and without Ca^{2+}. CaM-M13 is unpacked in the absence of Ca^{2+}, but FRET, which would cause depolarization of Venus, occurs. In contrast, CaM-M13 is packed, but there is no FRET. (d) Titration curve of the fluorescence anisotropy change of W-Cameleon, upon Ca^{2+} binding. Plots were fitted by Hill's equation.

form of photonic crystals, by the autocloning process [17,18]. The autocloning process enables fabrication of a multilayer structure, composed of a high-refractive index layer and low index layer, with each having triangular grooves. The multilayers have strong anisotropy, due to grooves. When the combined thickness of two adjacent layers is of the order of λ, then polarization-dependent passband or stopband takes place. If one of the two polarizations is stopped, while the other passes, we have a polarizer. On the other hand, if the combined thickness is much smaller than λ, then both polarizations are in the passband. This forms a waveplate property, which is due to the differences of the propagation phases. Usually, the autocloning requires a substrate, patterned by electron-beam lithography and dry etching (followed by bias sputtering of multilayers). The initial pattern is precisely conserved, if curved parallel grooves are initially formed and multilayers are successively deposited upon it. The polarizer used in this study had an extinction ratio of ~40 dB. The retardation error of the QWP was <4.5 degrees.

Development of homo-FRET microscopy

Our microscope possessed transmitted illumination, instead of epi-illumination, to reduce the depolarizing effects of dichroic mirrors. We measured the extinction factor, using a Glan–Thompson prism or photonic crystals, to determine if the photonic crystals could overcome the depolarization effect of high NA objective lens (60 × NA 1.40). As a result, the extinction factor obtained with high NA objective lens and the use of photonic crystals had a higher value (2543), compared to the Glan–Thompson prism (256). Thus, our homo-FRET microscopy may enable high dynamic range anisotropy measurement with high NA objective lens.

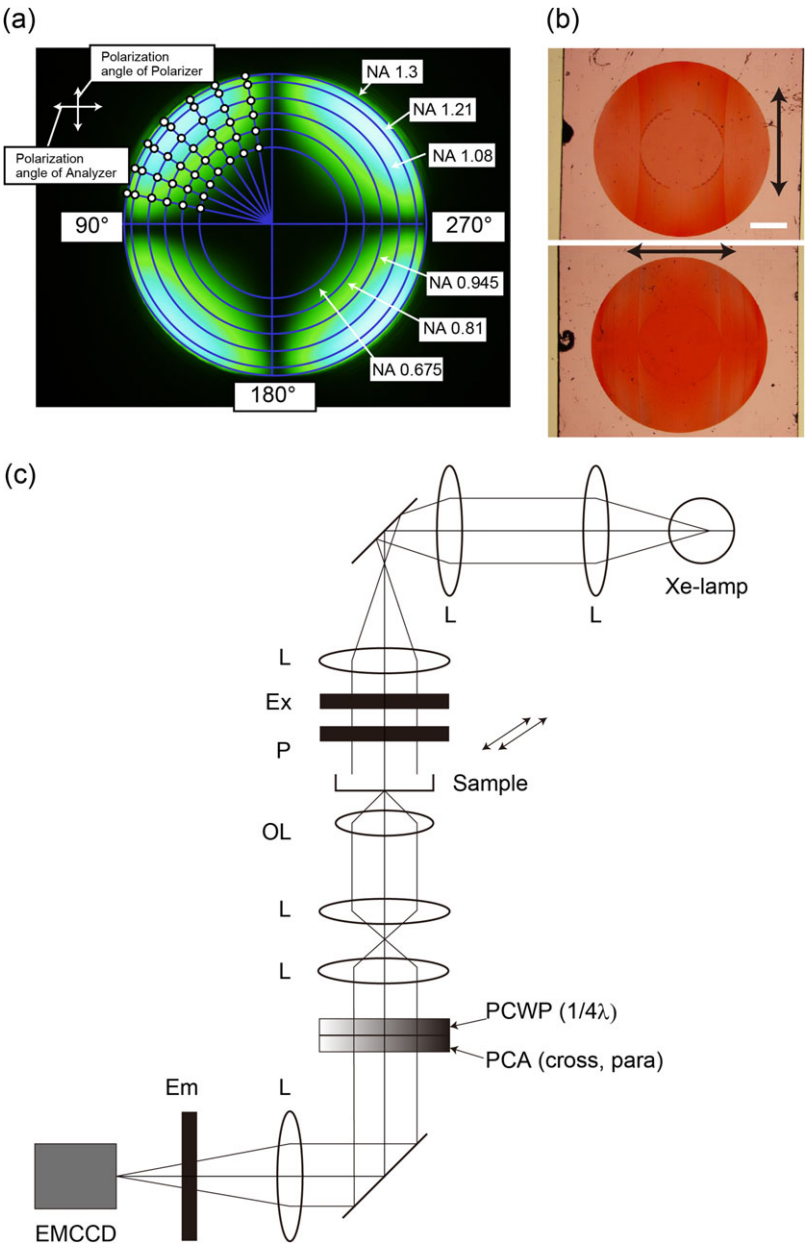

Fig. 2. Homo-FRET microscopy. (a) Conoscopic image, of objective lens, measured by the system shown in Supplementary data Fig. S2. (b) Bright field images of photonic crystal analyzers. Top: cross; Bottom: parallel. The arrows indicate the direction of the vibration axis. Scale bar is 1 mm. (c) Schematic drawing of homo-FRET microscopy. The fluorescence emission light is collected, by the objective lens, and is passed through the bottom port of the microscope. Photonic crystal analyzers were placed at the bottom of the microscope. Ex, Excitation filter wheel; P, polarize; OL, objective lens; PCWP; photonic crystal wave plate, PCA; photonic crystal analyzer; Em, Emission filter wheel.

Fluorescence anisotropy imaging of W-Cameleon

W-Cameleon was expressed in histamine-stimulated HeLa cells, to test its performance along with our photonic crystal base microscopy. W-Cameleon fluorescence anisotropy was measured with excitation at 472 nm and emission at 542 nm. Its fluorescence anisotropy value clearly increased after adding histamine; a Ca^{2+}-dependent oscillation was observed (Fig. 3a and b). Most of spikes beyond the 3σ (standard deviations) line indicating the significant difference from the background noise level. These results demonstrate that homo-FRET microscopy, with use of W-Cameleon, could be used for spatio-temporal visualization of changing Ca^{2+} concentrations in live cells, using only single emission color.

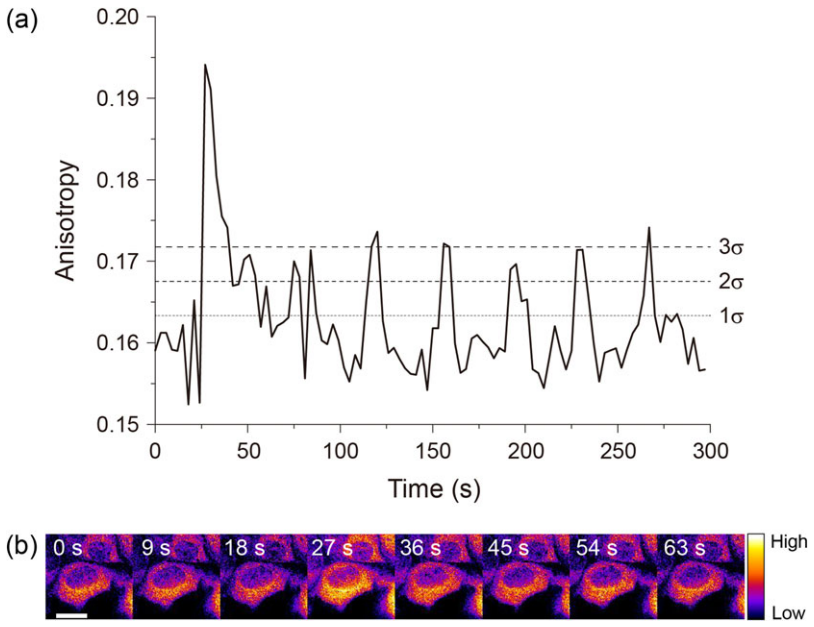

Fig. 3. Ca^{2+} oscillation by anisotropy change of W-Cameleon. (a) Time trajectory of W-Cameleon anisotropy change. Standards deviations (σ), 1σ (68%), 2σ (95%) and 3σ (99.7%) lines were calculated by using the data points before histamine stimulation. (b) Ratio image of W-Cameleon. Scale bar is 20 μm.

Multi-functional imaging of Ca^{2+}-activated, PKC-γ and MARCKS

Next, we examined the simultaneous imaging of multiple cellular events. We found that W-Cameleon, DsRedT3 fused with PKC-γ, and mSECFP, conjugated to the MARCKS, were observed simultaneously. PKC-γ is an isozyme of conventional PKC. Its functional C1 and C2 domains are bound to diacylglycol and Ca^{2+}, respectively, in its regulatory region [19]. Ca^{2+} activated PKC-γ translocates to the membrane [20]. MARCKS, one of the PKC substrates, binds to the plasma membrane, by inserting the hydrophobic myristate chain into the lipid bilayer. This causes an electrostatic interaction between basic residues from the effector domain and acidic phospholipids [21,22]. PKC-activated MARCKS translocates from the membrane to the cytoplasm. W-Cameleon, DsRedT3-conjugated PKC-γ and mSECFP-conjugated MARCKS were co-expressed in HeLa cells. The translocation of MARCKS, after the Ca^{2+} activation of PKC, was simultaneously visualized in living cells (Fig. 4a and b). MARCKS-mSECFP fluorescence was observed on the plasma membrane and PKC-γ-DsRedT3 in the cytosol, prior to histamine treatment. PKC-γ translocation was observed, in histamine-stimulated HeLa cells, with a W-Cameleon oscillatory change of anisotropy (Fig. 4a and b). MARKCS translocated from the plasma membrane to the cytosol and gradually accumulated in the perinuclear region, in a manner reciprocal to the behavior of PKC-γ (Fig. 4a and b). Thus, homo-FRET indicator, combined with homo-FRET microscopy, enabled simultaneous spatio-temporal imaging of multiple cellular functions in live single cells.

Discussion

In this paper, we demonstrated the performance of W-Cameleon, with the use of homo-FRET microscopy. The microscope was equipped with photonic crystals, to compensate for the depolarization effect of high NA objective lens. Our photonic crystals were designed for a particular objective lens, like the rectifier; therefore, they are not versatile. However, our polarization microscopy greatly improved the extinction factor. An electronically controlled liquid crystal-based polarizer would be useful, for versatile measurement of anisotropy with various objective lens [23]. Further investigation can be performed to improve polarization microscopy. The spatial resolution of homo-FRET microscopy with W-Cameleon was essentially same as the conventional wide-field fluorescence microscopy. On the other hand, because of the requirement of the changes of photonic crystals in every time points, we should note that the time resolution becomes slower than the hetero-FRET type indicators such as YC3.60 by simultaneous observation of donor and acceptor fluorescence with dual view optics. This drawback may influence to detect rapid Ca^{2+} change. Further improvement of optical system like dual view system would be desired.

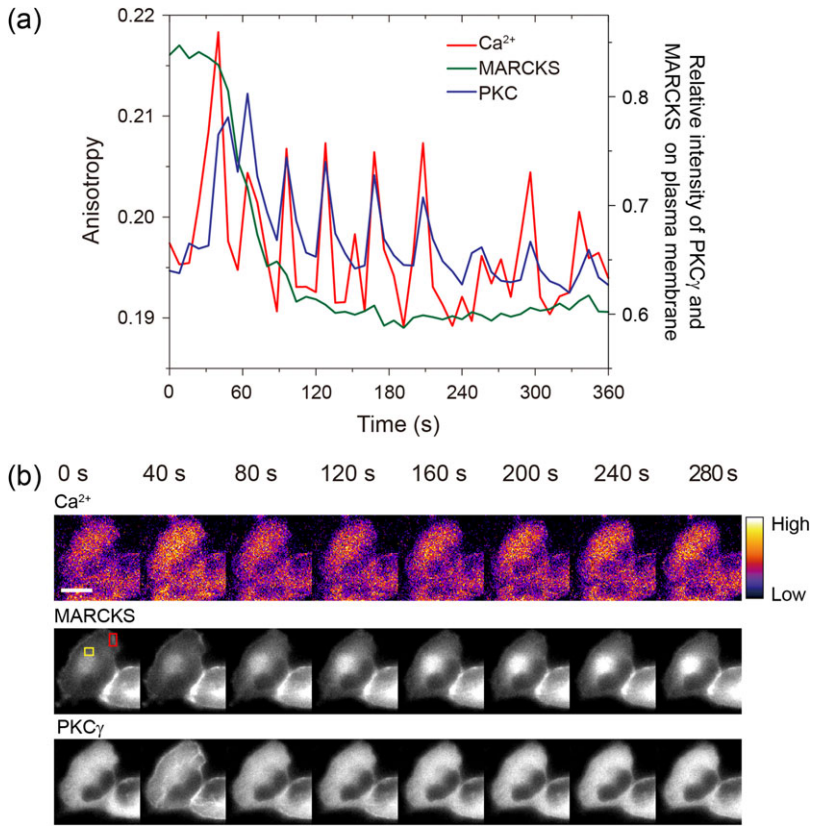

Fig. 4. Simultaneous observation of multiple cellular events. (a) Time trajectories of multiple cellular events of Ca^{2+}, PKC-γ and MARCKS, by W-Cameleon, DsRedT3-conjugated PKC-γ and mSECFP-conjugated MARCKS, respectively. Left vertical axis indicates the anisotropy change of W-Cameleon and right vertical axis indicates the relative intensity of PKC-γ and MARCKS, on the plasma membrane. (b) Montage images of W-Cameleon, DsRedT3-conjugated PKC-γ and mSECFP-conjugated MARCKS. Red and yellow region of interests indicated the cytosol and membrane region that were used for the ratio and relative intensities of (a). Scale bar is 10 μm.

In general, the fluorescent probe will likely be excited, when polarized light irradiates to a fluorescent probe, if the angle of absorption dipole moment of the fluorescent probes and the polarization of the excitation light are parallel. However, the angle of absorption and the acceptor emission dipole moments are not affected, by the angle of the excitation light polarization, when FRET occurs; this is due to the radiationless energy transfer from the donor to the acceptor. It explains why depolarization occurs by FRET. The titration curve, of W-Cameleon between Ca^{2+} concentration and anisotropy (Fig. 1d), clearly showed that depolarization occurred in the absence of Ca^{2+}. This indicated that the geometries of two Venus proteins were close enough to each other for FRET to take place. However, CaM-M13 is known to form a packed conformation, in the presence of Ca^{2+} [24]. Therefore, W-Cameleon indicated that FRET occurred, even in the absence of Ca^{2+}, but the CaM-M13 should be in an unpacked form. On the other hand, CaM-M13 should be in a packed form, in the presence of Ca^{2+}; whereas, fluorescence anisotropy increased, which indicated less FRET. Thus, we speculate that, in the presence of Ca^{2+}, CaM-M13 is packed. However, the geometry, of the donor emission dipole moment and acceptor absorption dipole moment, might be perpendicular, thus, preventing FRET to occur.

Simultaneous observation, of different molecular events, has become increasingly important for comprehensive understanding of the relationships. The applications, of dual-FRET-based biosensors or the Bimolecular Fluorescence Complementation (BiFC) -based FRET, have been developed as methods to simultaneously observe the interplay of multiple biological processes [25,26]. However, the dual-FRET-based simultaneous observation technique uses four different colors to detect only two different events, indicating a low cost performance approach. BiFC uses only one color and can effectively image multi-colors. However, BiFC is irreversible; therefore, it may not be suitable for observation of events that happen repeatedly. On the other hand, homo-FRET imaging only uses one color for detecting biological

events, such as Ca^{2+} oscillation. Thus, our homo-FRET-based indicator and homo-FRET microscopy will facilitate the observation of multiple cellular events.

Concluding remarks

This study demonstrated the homo-FRET imaging method, by using novel homo-FRET-based Ca^{+2} ion indicator, W-Cameleon and photonic crystal-based polarization fluorescence microscopy. Our method can expand the color hue, for simultaneous observation of multiple cellular events, by using fluorescence imaging quantitatively.

Supplementary data

Supplementary data are available at *Journal of Microscopy* online.

Acknowledgements

We thank Dr N. Saito for providing MARCKS-GFP gene. We also thank Dr T. Matsuda for technical supports.

Funding

Scientific Research on Innovative Areas; 'Spying minority in biological phenomena (No. 3306)'; from the Ministry of Education, Culture, Sports, Science and Technology; Japan (No. 23115003); and partly supported by Core Research for Evolution Science and Technology (CREST); Japan Science and Technology Agency (JST) (to T.N.).

Conflict of interest

The authors declare no competing interests exist.

References

1. Zhao Y, Araki S, Wu J, Vignali K M, Dilioglou S, Vanin E F, and Vignali D A (2011) An expanded palette of genetically encoded Ca^{2+} indicators. *Science* 333: 1888–1891.
2. Nagai T, Yamada S, Tominaga T, Ichikawa M, and Miyawaki A (2004) Expanded dynamic range of fluorescent indicators for Ca(2+) by circularly permuted yellow fluorescent proteins. *Proc. Natl. Acad. Sci. U S A* 101: 10554–10559.
3. Szymczak A L, Workman C J, Wang Y, Vignali K M, Dilioglou S, Vanin E F, and Vignali D A (2004) Correction of multi-gene deficiency in vivo using a single 'self-cleaving' 2A peptide-based retroviral vector. *Nat. Biotechnol.* 22: 589–594.
4. Arai Y, and Nagai T (2013) Extensive use of FRET in biological imaging. *Microscopy (Oxf)* 62: 419–428.
5. Weber G (1954) Dependence of the polarization of the fluorescence on the concentration. *Trans. Faraday Soc.* 50: 552–555.
6. Bastiaens P I, and Squire A (1999) Fluorescence lifetime imaging microscopy: spatial resolution of biochemical processes in the cell. *Trends Cell Biol.* 9: 48–52.
7. Blackman S M, Piston D W, and Beth A H (1998) Oligomeric state of human erythrocyte band 3 measured by fluorescence resonance energy homotransfer. *Biophys J.* 75: 1117–1130.
8. Runnels L W, and Scarlata S F (1995) Theory and application of fluorescence homotransfer to melittin oligomerization. *Biophys J.* 69: 1569–1583.
9. Varma R, and Mayor S (1998) GPI-anchored proteins are organized in submicron domains at the cell surface. *Nature* 394: 798–801.
10. Gautier I, Tramier M, Durieux C, Coppey J, Pansu R B, Nicolas J C, Kemnitz K, and Coppey-Moisan M (2001) Homo-FRET microscopy in living cells to measure monomer-dimer transition of GFP-tagged proteins. *Biophys J.* 80: 3000–3008.
11. Tramier M, and Coppey-Moisan M (2008) Fluorescence anisotropy imaging microscopy for homo-FRET in living cells. *Methods Cell Biol.* 85: 395–414.
12. Bahlmann K, and Hell S W (2000) Electric field depolarization in high aperture focusing with emphasis on annular apertures. *J. Microsc.* 200: 59–67.
13. Inoue S, and Hyde W L (1957) Studies on depolarization of light at microscope lens surfaces. II. The simultaneous realization of high resolution and high sensitivity with the polarizing microscope. *J. Biophys. Biochem. Cytol.* 3: 831–838.
14. Sato T, Araki T, Sasaki Y, Tsuru T, Tadokoro T, and Kawakami S (2007) Compact ellipsometer employing a static polarimeter module with arrayed polarizer and wave-plate elements. *Appl. Opt.* 46: 4963–4967.
15. Saito K, Kobayashi K, Tani T, and Nagai T (2008) A mercury arc lamp-based multi-color confocal real time imaging system for cellular structure and function. *Cell Struct. Funct.* 33: 133–141.
16. Kajihara D, Abe R, Iijima I, Komiyama C, Sisido M, and Hohsaka T (2006) FRET analysis of protein conformational change through position-specific incorporation of fluorescent amino acids. *Nat. Methods* 3: 923–929.
17. Kawakami S (1997) Fabrication of submicrometre 3D periodic structures composed of Si/SiO2. *Electron. Lett.* 33: 1260–1261.
18. Kawashima T, Miura K, Sato T, and Kawakami S (2000) Self-healing effects in the fabrication process of photonic crystals. *Appl. Phys. Lett.* 77: 2613–2615.
19. Nishikawa K, Toker A, Johannes F J, Songyang Z, and Cantley L C (1997) Determination of the specific substrate sequence motifs of protein kinase C isozymes. *J. Biol. Chem.* 272: 952–960.
20. Sakai N, Sasaki K, Ikegaki N, Shirai Y, Ono Y, and Saito N (1997) Direct visualization of the translocation of the gamma-subspecies of protein kinase C in living cells using fusion proteins with green fluorescent protein. *J. Cell Biol.* 139: 1465–1476.
21. Kim J, Shishido T, Jiang X, Aderem A, and McLaughlin S (1994) Phosphorylation, high ionic strength, and calmodulin reverse the binding of MARCKS to phospholipid vesicles. *J. Biol. Chem.* 269: 28214–28219.
22. Ohmori S, Sakai N, Shirai Y, Yamamoto H, Miyamoto E, Shimizu N, and Saito N (2000) Importance of protein kinase C targeting for the phosphorylation of its substrate, myristoylated alanine-rich C-kinase substrate. *J. Biol. Chem.* 275: 26449–26457.

23. Kozawa Y, Hibi T, Sato A, Horanai H, Kurihara M, Hashimoto N, Yokoyama H, Nemoto T, and Sato S (2011) Lateral resolution enhancement of laser scanning microscopy by a higher-order radially polarized mode beam. *Opt. Express* 19: 15947–15954.
24. Miyawaki A, Llopis J, Heim R, McCaffery J M, Adams J A, Ikura M, and Tsien R Y (1997) Fluorescent indicators for Ca2+ based on green fluorescent proteins and calmodulin. *Nature* 388: 882–887.
25. Ai H W, Hazelwood K L, Davidson M W, and Campbell R E (2008) Fluorescent protein FRET pairs for ratiometric imaging of dual biosensors. *Nat. Methods* 5: 401–403.
26. Shyu Y J, Suarez C D, and Hu C D (2008) Visualization of AP-1 NF-kappaB ternary complexes in living cells by using a BiFC-based FRET. *Proc. Natl. Acad. Sci. USA* 105: 151–156.